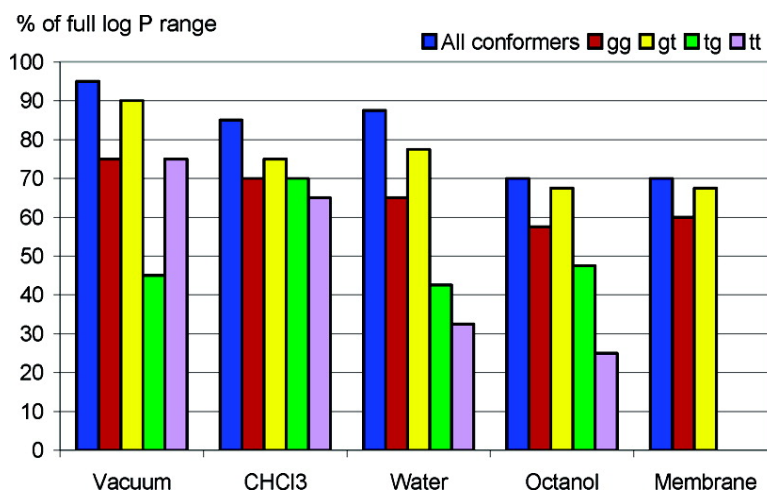


Solvent Constraints on the Property Space of Acetylcholine. 2. Ordered Media

Giulio Vistoli, Alessandro Pedretti, Luigi Villa, and Bernard Testa

J. Med. Chem., **2005**, 48 (22), 6926-6935 • DOI: 10.1021/jm0580306 • Publication Date (Web): 04 October 2005

Downloaded from <http://pubs.acs.org> on March 29, 2009



More About This Article

Additional resources and features associated with this article are available within the HTML version:

- Supporting Information
- Links to the 1 articles that cite this article, as of the time of this article download
- Access to high resolution figures
- Links to articles and content related to this article
- Copyright permission to reproduce figures and/or text from this article

[View the Full Text HTML](#)

Solvent Constraints on the Property Space of Acetylcholine. 2. Ordered Media

Giulio Vistoli,^{*,†} Alessandro Pedretti,[†] Luigi Villa,[†] and Bernard Testa[‡]

Istituto di Chimica Farmaceutica, Facoltà di Farmacia, Università di Milano, Viale Abruzzi 42, I-20131 Milano, Italy, and Department of Pharmacy, University Hospital Centre (CHUV), Rue du Bugnon, CH-1011 Lausanne, Switzerland

Received May 25, 2005

The objective of this study was to investigate the conformational and property spaces of acetylcholine in hydrated octanol and in a membrane model. Molecular dynamics simulations of long duration (15 ns) were carried out, yielding 3000 conformers. For each, we calculated N⁺–C8 distance, solvent-accessible surface area (SAS), polar surface area (PSA), dipole moment, and lipophilicity (virtual logP). Their variations as a function of the dihedral angles τ_2 and τ_3 remained unexpectedly broad and comparable to those seen previously in a vacuum, in water, and in chloroform.¹² Thus, each of the seven conformational clusters was able to access a marked proportion of the lipophilicity space accessible to acetylcholine (0.40 in the logP scale). Histograms of logP distributions revealed two overlapping populations, namely more lipophilic and more hydrophilic. Their deconvolution into two Gaussian curves demonstrated solvent-mediated constraints on the lipophilicity space of acetylcholine, clearly showing how a polar medium favors polar conformers, whereas the opposite is true for media of low polarity.

Introduction

Since the emergence of combinatorial chemistry and chemical libraries, great attention is being paid to the concepts of chemical diversity and chemical space.¹ The usual methods to approach a quantitative description of chemical space is first to calculate a number of structural and physicochemical descriptors for each compound, e.g. molecular mass, number of atoms, number of rotatable bonds, charges, and some molecular properties such as a fragment-based logP.² In a second step, multivariate analysis such as PCA (principal component analysis) allows a multidimensional hyperspace to be constructed, with each compound characterized by a single set of coordinates. Display is usually two-dimensional (using principal compounds **1** and **2**) or three-dimensional.

Whereas this approach has proven very successful in comparing chemical libraries and designing combichem series, it nevertheless is based on the assumption that the molecular properties being computed are discrete and invariant. This assumption derives from the restrictions imposed by the handling of huge databases, but like many assumptions it tends to fade in the background and be taken as fact. Yet as chemistry progresses, so does our understanding of molecular structure taken in its broadest sense, namely the mutual interdependence between geometric features and physicochemical properties.³ Some of the geometric features of a given compound are invariant, namely its configuration and usually its connectivity (tautomerism excepted), whereas others can vary within a given range, e.g., its conformation.^{4,5} The conformational behavior of molecules as assessed experimentally or computationally can be expressed in conformational hypersurfaces, and the ensemble of all conformers of a

given compound is often taken as defining a conformational space.

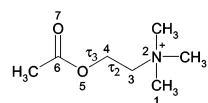
What is more, powerful computational methods based in particular on molecular interaction fields (MIFs) now allow some physicochemical properties to be computed for each conformer. Such methods include MEPs (molecular electrostatic potentials) which encode electrostatic forces,⁶ MLPs (molecular lipophilicity potentials) which encode hydrophobicity, H-bonding capacity and polarizability,^{7,8} and the more recent MHBPs (molecular hydrogen-bonding potentials⁹). MLPs are of particular relevance in the context of this study, since they allow to back-calculate the partition coefficient of a given molecule.^{7,8} Because all 3D-MIFs are strongly dependent on the 3D-geometry of the investigated molecules (i.e. their conformational state), researchers are able to calculate a “virtual” logP for each conformer,⁷ a computational achievement that has received experimental validation. Indeed, there is experimental evidence that “rigidified” conformers (i.e., mainly diastereomers) differ in their logP values.¹⁰ Recent NMR kinetic studies have afforded a direct proof that conformers differ in their octanol/water partition coefficient.¹¹

Since a virtual logP can be computed for each conformer in the conformational space of a molecule, a lipophilicity space must correspond to the conformational space. In a previous work,¹² we investigated the property space of acetylcholine. This molecule was chosen as the object of study given its interesting molecular structure, major biological significance, and the many data (experimental and computational) accumulated on its conformational behavior.^{13–26} Molecular dynamics simulations of long duration (30 ns) were carried out with acetylcholine in a vacuum or in a box of solvent (chloroform, water, water plus one chloride counterion). For each of the 6000 conformers stored during each run, various geometric and physicochemical properties were calculated, namely the N⁺–C8 distance, solvent-accessible surface area (SAS), polar surface

* Corresponding author. Tel +39 02 50317545; Fax +39 02 50317565; e-mail: Giulio.Vistoli@unimi.it.

[†] Università di Milano.

[‡] University Hospital Centre (CHUV).



$$\tau_1 = \text{C1-N2-C3-C4}$$

$$\tau_2 = \text{N2-C3-C4-O5}$$

$$\tau_3 = \text{C3-C4-O5-C6}$$

$$\tau_4 = \text{C4-O5-C6-O7}$$

distance monitored = N2-C8

Figure 1. Dihedral angles in acetylcholine. Their values are defined according to Klyne and Prelog.⁵

area (PSA), dipole moment, and lipophilicity (virtual logP). The variations of these properties as a function of the dihedral angles τ_2 and τ_3 were unexpectedly broad for such a small molecule. Dipole moment and virtual logP were well correlated, and they varied in a complex, yet well understandable, manner with the dihedral angles. For example, each of the seven conformational clusters was able to access much of the lipophilicity space of acetylcholine. Solvent constraints on the property space clearly indicated that a polar medium tends to favor polar conformers, whereas the opposite is true for a solvent of low polarity.

In the present work, we investigated the conformational and property spaces of acetylcholine in a well-ordered (anisotropic) medium, namely a phosphatidylcholine membrane model. Hydrated *n*-octanol (1 mol water/4 mol octanol) was also used to represent a medium structurally intermediate between a membrane and the isotropic solvents previously used. The objective of this study was thus to gain a global and quantitative view of the influence (i.e., constraints) of diverse media (from a vacuum to a membrane) on the conformational and property spaces of acetylcholine. The geometric properties calculated for each conformer were the dihedral angles τ_2 and τ_3 and the distance between N⁺ and C8 (Figure 1). The physicochemical properties again included lipophilicity (logP), dipole moment, polar surface area (PSA), and solvent accessible surface (SAS) which is a mixed geometric and physicochemical property. The results should be of value when reflecting on the behavior of compounds in biological systems, e.g. when they permeate membranes or bind to biological targets such as enzymes and receptors.

Results and Discussion

Conformational Behavior of Acetylcholine in *n*-Octanol and a Membrane. The conformational space of acetylcholine was simulated during 15 ns in hydrated octanol (molar ratio 1/4) and in a membrane model. The 3000 conformers so recorded are displayed in Figures 2B and 2C, respectively. To put these results into perspective, we present in Figure 2A the conformational behavior of acetylcholine in a vacuum (30 ns, 6000 conformers), which reveals a very different behavior. Whereas in both media τ_3 showed no clear preference in the range 60° to 300°, τ_2 was mostly *antiperiplanar* in hydrated octanol (as seen in Figure 2B) and exclusively *gauche* in membrane model (as seen in Figure 2C).

The quantitative differences are presented in Table 1, which compares the relative abundance of each conformational cluster as monitored in the five media

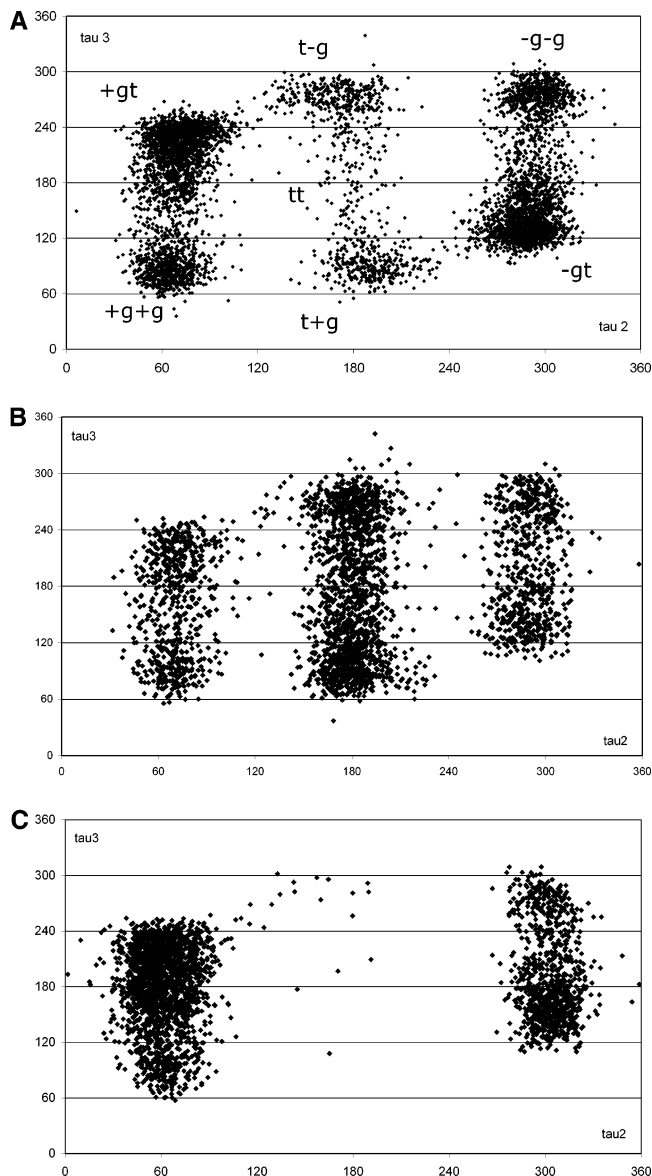


Figure 2. The conformational behavior of acetylcholine (τ_2 vs τ_3 plot) as revealed by MD simulations. A: In a vacuum (30 ns, 6000 conformers).¹² B: In hydrated octanol (15 ns, 3000 conformers). C: In a membrane model (15 ns, 3000 conformers).

considered in the previous¹² and present study (namely vacuum, chloroform, water, octanol, and membrane). When analyzing the relative abundance of each conformational cluster in isotropic media, one observes a significant increase in all extended geometries (i.e. with τ_2 in trans, tg and tt) compared to a vacuum, and a corresponding decrease of the gt clusters but not of the gg clusters, whose abundance seems quite insensitive to the medium. The increase in extended conformers becomes even more evident in octanol, where their proportion is higher than in all other media (Table 1). The same is true of the transitional forms (38%), suggesting that acetylcholine experiences a slowing down of intramolecular motions due to the elongated size of the solvent.²⁷

In our previous study with simple isotropic solvents,¹² three main factors were considered to explain solvent effects, namely intrinsic polarity, solute-solvent interactions, and friction. However, these factors alone

Table 1. Relative Abundance of Conformer in Each Conformational Cluster (in %), as Accumulated during 30 ns or 15 ns MD Simulations

conformational cluster ($\tau_2\tau_3$)	medium				
	vacuum ($\epsilon = 1$) (30 ns) ^a	chloroform (30 ns) ^a	water (30 ns) ^a	hydrated <i>n</i> -octanol (15 ns)	membrane model (15 ns)
+g+g	12.1	9.3	12.3	9.0	15.7
-g-g	12.1	12.8	13.3	10.2	9.4
+gt	29.9	15.1	15.4	10.1	50.3
-gt	27.0	17.8	16.1	10.0	21.4
t+g	2.5	8.2	3.6	6.7	0
t-g	2.5	7.4	3.8	7.4	0
tt	1.1	4.1	9.3	8.7	0
gg + gt	80.8	55.5	57.3	39.3	96.8
tg + tt	6.4	19.7	16.7	22.8	0
anticlinal (transitional) forms	12.8	24.8	26.0	37.8	3.2

^a Results from a previous study.¹²

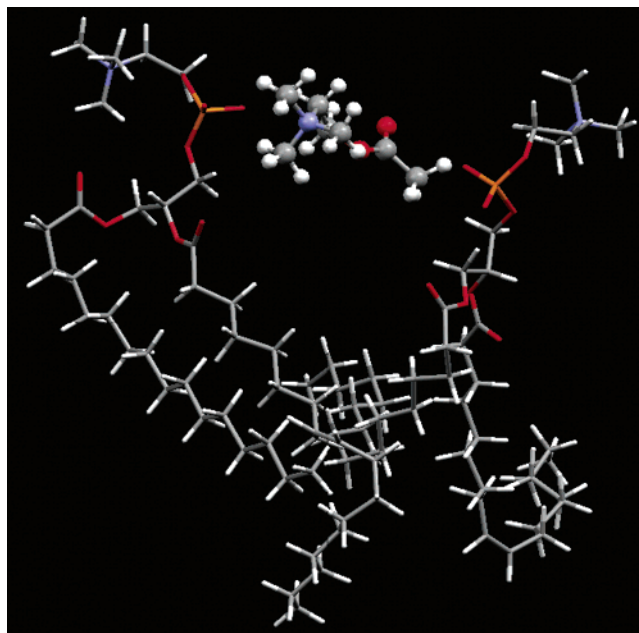
appear unable to account for the remarkable abundance of extended conformers in hydrated octanol. Clearly, hydrogen bonds between the ester group of acetylcholine and a hydroxy group of *n*-octanol or water contribute to the abundance of extended conformers, but they cannot account for a relative abundance greater than that found in water. We postulate that solvent size and shape should be considered as a fourth factor. Indeed, when the size and shape of solvent becomes comparable with that of the solute (e.g. acetylcholine and octanol), the solute minimizes steric repulsion by mimicking the shape of the solvent.²⁷ Here, the extended conformers of acetylcholine can successfully mimic the preferred zigzag conformation of octanol.

In our membrane model, the extended geometries of acetylcholine disappeared totally (Figure 2C), as τ_2 never assumed trans conformations. The 3000 conformers were almost exclusively distributed among gg and gt clusters, and transitional forms were practically absent. Importantly, we checked that this particular conformational profile is independent of the starting conformation, since identical results were observed when starting with a fully extended tt conformer (results not shown).

Table 2. Limits (first rows), Ranges (second rows), and Mean Values \pm 99.9% CL (third rows) of the Molecular Properties of Acetylcholine Conformers Generated during MD Simulations

property	medium ^a				
	vacuum ($\epsilon = 1$)	chloroform	water	octanol	membrane
distance ^b	4.37 to 6.39	4.35 to 6.37	4.37 to 6.36	4.43 to 6.38	4.30 to 6.20
	2.02	2.02	1.99	1.95	1.90
	5.25 \pm 0.009	5.40 \pm 0.017	5.43 \pm 0.019	5.57 \pm 0.027	5.06 \pm 0.014
SAS ^c	343 to 377	336 to 376	341 to 378	335 to 374	337 to 371
	34	40	37	39	34
	358 \pm 0.21	356 \pm 0.25	361 \pm 0.30	358 \pm 0.42	354 \pm 0.30
PSA ^d	24.2 to 44.0	28.5 to 50.4	24.4 to 44.8	32.0 to 51.1	30.1 to 49.3
	20.0	21.9	20.4	19.1	19.2
	35.0 \pm 0.12	40.1 \pm 0.16	37.8 \pm 0.11	42.7 \pm 0.20	40.7 \pm 0.14
logP _{oct} ^e	-2.53 to -2.15	-2.53 to -2.19	-2.55 to -2.20	-2.52 to -2.24	-2.51 to -2.23
	0.38	0.34	0.35	0.28	0.28
	-2.34 \pm 0.0026	-2.36 \pm 0.0026	-2.42 \pm 0.0026	-2.40 \pm 0.0030	-2.39 \pm 0.0030
dipole moment	5.51 to 10.1	7.43 to 9.54	7.80 to 9.71	7.63 to 9.45	7.56 to 9.40
	4.50	2.07	1.91	1.88	1.84
	7.78 \pm 0.035	8.40 \pm 0.016	8.88 \pm 0.014	8.67 \pm 0.020	8.66 \pm 0.019

^a In each box, the first line shows the limits (minimum to maximum value), the second line the range, and the third line the mean \pm 99.9% confidence limits (t test). The results for a vacuum, chloroform, and water are from a previous study.¹² ^b Distance in Å between (N⁺) and (OC)CH₃. ^c Solvent-accessible surface area in Å². ^d Polar surface area in Å². ^e "Virtual" logP calculated by the molecular lipophilicity potential.

**Figure 3.** Interactions of acetylcholine in a membrane model (water molecules are not displayed for greater clarity).

The complete absence of extended conformers in a membrane model can be explained by the fact that only the folded conformers of acetylcholine can simultaneously create strong electrostatic interactions of their ammonium group with a phosphate in the membrane and minimize the repulsion between their ester group and another phosphate (Figure 3). While in all other media the conformational profile of acetylcholine was heavily solvent-dependent, all seven possible conformational clusters were always present (Table 1). The membrane environment is thus the only one so far where some conformational clusters (i.e., the tg and tt clusters) disappear entirely, due as explained above to solute-solvent interactions being predominant over intrasolute interactions.

While in all other media the conformational profile of acetylcholine showed a centrosymmetric distribution around the full-extended tt cluster and three pairs of

Table 3. Mean Solvent-Accessible Surface Area (SAS) Values, Mean Polar Surface Area (PSA) Values, and Mean logP Values, \pm SD (first rows) and Ranges (second rows) for the Seven Conformational Clusters of Acetylcholine As Generated during MD Simulations

(A) Mean Solvent-Accessible Surface Area (SAS) Values \pm SD (first rows) and Ranges (second rows)					
conformational cluster ($\tau_2\tau_3$)	medium ^a				
	vacuum ($\epsilon = 1$)	chloroform	water	octanol	membrane
+g+g	357 \pm 5 26	352 \pm 5 26	357 \pm 5 27	352 \pm 5 25	354 \pm 5 30 30
-g-g	357 \pm 5 25	352 \pm 5 27	357 \pm 5 27	352 \pm 5 24	352 \pm 5 26
+gt	357 \pm 5 25	352 \pm 5 28	357 \pm 5 26	353 \pm 5 24	354 \pm 5 30 30
-gt	357 \pm 5 28	352 \pm 5 28	357 \pm 5 26	353 \pm 5 23	353 \pm 5 26 26
t+g	362 \pm 3 18	358 \pm 4 20	363 \pm 3 16	359 \pm 3 13	-
t-g	363 \pm 3 14	359 \pm 3 21	363 \pm 3 20	359 \pm 3 23	-
tt	373 \pm 2 10	367 \pm 3 14	371 \pm 3 13	374 \pm 2 10	-

(B) Mean Polar Surface Area (PSA) Values \pm SD (first rows) and Ranges (second rows)					
conformational cluster ($\tau_2\tau_3$)	medium ^b				
	vacuum ($\epsilon = 1$)	chloroform	water	octanol	membrane
+g+g	34.8 \pm 2.03 13.9	38.1 \pm 2.99 16.9	36.2 \pm 1.64 10.6	40.2 \pm 2.15 12.4	40.8 \pm 1.95 12.1
-g-g	34.6 \pm 1.97 12.2	38.4 \pm 2.87 17.6	36.2 \pm 1.58 12.4	40.0 \pm 1.97 12.4	39.8 \pm 2.35 13.1
+gt	34.6 \pm 2.57 16.9	42.6 \pm 3.45 18.0	36.8 \pm 2.11 15.1	40.3 \pm 2.36 14.2	40.7 \pm 2.36 13.8
-gt	34.7 \pm 2.69 16.91	42.7 \pm 3.45 19.2	36.7 \pm 1.95 16.2	40.3 \pm 2.50 14.8	41.3 \pm 2.24 14.0
t+g	35.9 \pm 2.34 12.1	38.4 \pm 2.83 15.6	38.1 \pm 2.23 12.1	43.5 \pm 2.23 14.3	-
t-g	36.2 \pm 2.59 11.1	38.4 \pm 2.73 16.3	38.1 \pm 2.13 12.5	43.3 \pm 2.51 14.9	-
tt	40.6 \pm 1.13 5.41	43.6 \pm 2.75 15.6	40.4 \pm 1.21 7.94	46.2 \pm 1.34 6.83	-

(C) Mean logP Values \pm SD (first rows) and Ranges (second rows)					
conformational cluster ($\tau_2\tau_3$)	medium ^c				
	vacuum ($\epsilon = 1$)	chloroform	water	octanol	membrane
+g+g	-2.36 \pm 0.05 0.28	-2.34 \pm 0.05 0.28	-2.40 \pm 0.05 0.25	-2.39 \pm 0.04 0.20	-2.40 \pm 0.04 0.24
-g-g	-2.36 \pm 0.05 0.30	-2.35 \pm 0.06 0.28	-2.40 \pm 0.05 0.26	-2.39 \pm 0.05 0.23	-2.39 \pm 0.05 0.22
+gt	-2.33 \pm 0.07 0.33	-2.37 \pm 0.06 0.29	-2.39 \pm 0.06 0.31	-2.39 \pm 0.05 0.27	-2.39 \pm 0.05 0.26
-gt	-2.33 \pm 0.07 0.36	-2.37 \pm 0.06 0.30	-2.39 \pm 0.06 0.30	-2.39 \pm 0.05 0.24	-2.39 \pm 0.05 0.27
t+g	-2.33 \pm 0.04 0.17	-2.36 \pm 0.06 0.28	-2.37 \pm 0.04 0.20	-2.36 \pm 0.03 0.16	-
t-g	-2.34 \pm 0.04 0.18	-2.36 \pm 0.06 0.28	-2.36 \pm 0.03 0.17	-2.35 \pm 0.03 0.19	-
tt	-2.47 \pm 0.02 0.10	-2.40 \pm 0.06 0.26	-2.48 \pm 0.02 0.13	-2.40 \pm 0.02 0.10	-

^a In each box, the first line shows the mean \pm SD, the second line the range. The results for a vacuum, chloroform and water are from a previous study.¹² ^b In each box, the first line shows the mean \pm SD and the second line the range. ^c In each box, the first line shows the mean \pm SD and the second line the range.

chiral conformational clusters having practically identical relative abundance (namely +g+g \cong -g-g; +gt \cong -gt, and t+g \cong t-g), the same was far from true in a membrane. Indeed, the membrane was found to break these symmetries, with +g+g and +gt being twice as abundant as -g-g and -gt. This particular profile is explainable by the membrane being an anisotropic and chiral medium (POPC is a chiral molecule) able to induce chiral conformations by interacting preferentially with the +g+g and +gt conformers and thus shifting the equilibrium in their favor.

An Overview of the Property Space of Acetylcholine in Octanol and a Membrane. A number of geometric and physicochemical properties were calculated for each of the 3000 conformers stored during the 15 ns simulations in hydrated octanol and in the membrane model. The results are compiled in Table 2, where they are compared with the corresponding values obtained in a vacuum, in water, and in chloroform.¹²

The simulations in octanol and membrane confirm some trends already observed in the previous study,¹² that the physicochemical properties related to polarity

Table 4. Pairwise Squared Correlation Matrix (r^2) for the Molecular Properties Considered Here

property ^a	logP ^b					dipole moment ^b					PSA ^b					SAS ^b				
dipole moment	0.77	0.81	0.76	0.78	0.74															
PSA	0.47	0.46	0.29	0.29	0.11	0.58	0.60	0.36	0.44	0.28										
SAS	0.39	0.41	0.42	0.34	0.36	0.40	0.52	0.43	0.46	0.38	0.35	0.56	0.41	0.54	0.10					
distance	0.13	0.16	0.24	0.14	0.17	0.08	0.21	0.19	0.19	0.12	0.14	0.42	0.35	0.47	0.01	0.72	0.74	0.85	0.80	0.68

^a See Table 2 for definition and units. ^b First column, r^2 for values in vacuo, second column for values in chloroform, third column for values in water, fourth column for values in octanol, and fifth column for values in a membrane. The best correlations (≥ 0.60) are boldface.

and lipophilicity span markedly broad ranges, whereas the geometric properties span more limited ranges. Table 2 shows that the effects of solvents on the property ranges are quite similar. This is particularly remarkable in a membrane where ranges decrease very little when compared to a vacuum, although the conformational space is severely constrained.

The spaces of distance, SAS, and PSA showed unre-markable and presumably nonsignificant variations among the five media. In contrast, the dipole moment and most notably the lipophilicity space are different in a vacuum compared to any of the physical media. Indeed, the polarity of acetylcholine is increased in all solvents and in the membrane compared to a vacuum; although the differences in the mean logP values are very small, they are significant as assessed by their 99.9% CL. Nevertheless, a basically different approach (i.e., a deconvolution of histograms, see later) will allow a better analysis.

Tables 3 show how the media influence the mean SAS (Table 3A), mean PSA (Table 3B), and mean logP (Table 3C) values in each conformational cluster. For example, the SAS averages in octanol show that the folded conformers (gg and gt clusters), which cannot mimic the shape of the solvent molecules, have the lowest values to minimize friction with the solvent, while the extended (tt) conformers have the highest SAS values to maximize mimicry with the solvent. The SAS values of folded conformers are also lowest in a membrane, confirming the key role of friction. In contrast, mean PSA values show more homogeneous trends such that they are always higher in octanol or a membrane than in water or a vacuum. This is explained by the important role of polar solute–solvent interactions in these media. The mean logP values in Table 3C show a very interesting profile, especially in octanol. Indeed and in relative terms, they are at intermediate or high levels in octanol for folded conformers and lowest in the tt cluster. It is very intriguing to note that acetylcholine can modulate the properties of its fully extended conformers in an apparently contrasting way, selecting conformers that are simultaneously the most extended ones to better mimic the shape of the solvent, and the most lipophilic ones to preserve an intermediate polarity. In a membrane, acetylcholine shows mean logP values very similar to those in water; this is best understood considering that the compound does not move away from the polar phospholipid heads during the entire duration of the simulations. Taken globally, these results confirm one of the most interesting conclusions of the first study:¹² that each cluster of conformers spans most of the property space of acetylcholine.

The pairwise correlations of parameters (Table 4) in octanol and in a membrane are generally in good agreement with those for a vacuum, water, and chloro-

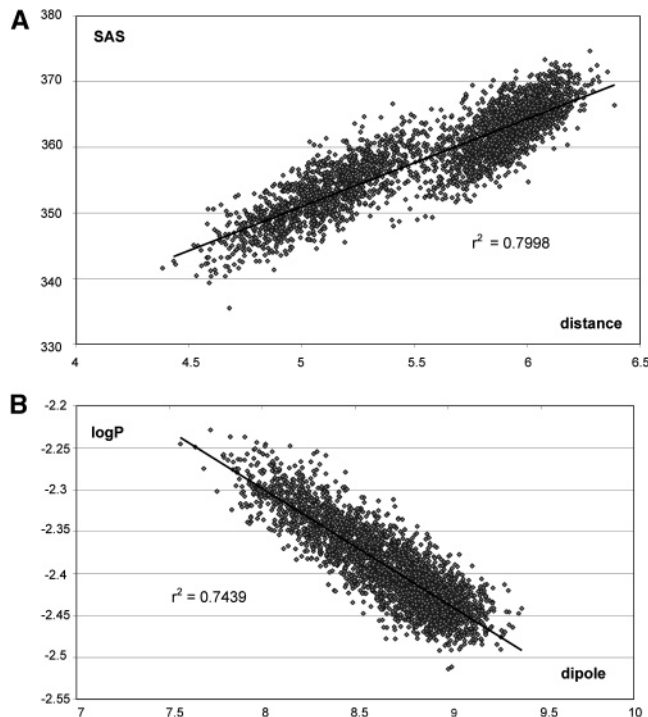


Figure 4. Relations between some of the parameters computed in octanol and a membrane. A: Correlation between the solvent-accessible surface area (SAS) and the distance between (N^+) and $(OC)CH_3$ in octanol ($r^2 = 0.80$). B: Correlation between logP (calculated by the molecular lipophilicity potential⁸) and the dipole moment in a membrane ($r^2 = 0.74$).

form. With some previously mentioned exceptions,¹² no pair of parameters shows a strong linear correlation (i.e., most r^2 are < 0.6). One interesting exception is the correlation between two geometric parameters, distance, and SAS ($r^2 = 0.80$ in octanol, Figure 4A, and 0.68 in a membrane). The other, and more noteworthy correlation is between dipole moment and logP, whose r^2 values are equal to 0.78 in octanol and 0.74 in a membrane (Figure 4B).

Overall, Table 4 shows that the correlation coefficients in a membrane tend to be lower than in other media, but otherwise they appear quite independent from the conditions. The sole exception involves the relation between dipole moment and PSA, which are fair only in very apolar media only (vacuum, $r^2 = 0.58$; chloroform, $r^2 = 0.60$). One can conclude that this relation is best in media that do not restrict the conformational space of acetylcholine, and that it loses significance in media that constrain the conformational profile (mainly the membrane).

The variation of physicochemical properties with both τ_2 and τ_3 is best illustrated in 3D-plots (Figures 5). The plots for octanol and a membrane, as obtained in this work, show marked similarities but some differences

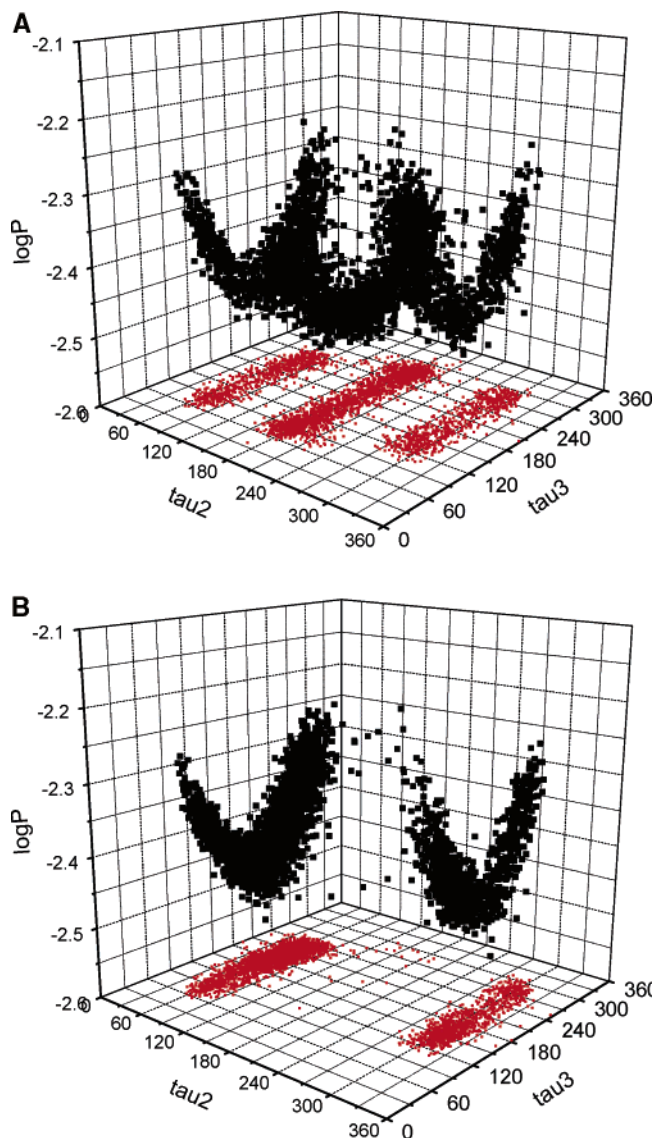


Figure 5. 3D-plots of virtual logP vs τ_2 and τ_3 . A: In hydrated *n*-octanol. B: In a membrane model.

with those obtained in vacuo, chloroform, and water.¹² Here again, lipophilicity was not influenced by variations in τ_2 but was very sensitive to variations in τ_3 , with the most lipophilic conformers having $\tau_3 = \text{gauche}$, and the most hydrophilic having $\tau_3 = \text{trans}$ (Figure 5A and 5B for octanol and a membrane, respectively). In agreement with τ_2 vs. τ_3 plots (Figure 2B and 2C), the 3D-plot for octanol (Figure 5A) is most populated for $\tau_2 = \text{trans}$, as a result of the great abundance of extended acetylcholine conformers in hydrated octanol. In a membrane (Figure 5B) only conformers with $\tau_2 = \text{gauche}$ exist, yet one sees again that the range of lipophilicities covered by acetylcholine in the two media remains identical. Given the high inverse relation between lipophilicity and dipole moment, it comes as no surprise that 3D-plots of dipole vs τ_2 and τ_3 are mirror images of the 3D-plots of the dipole moment (results not shown).

Solvent Constraints on the Lipophilicity Space of Acetylcholine. The data reported herein and previously¹² reveal modest differences in ranges and mean values of properties computed in the various media. As seen in Table 2, the medium slightly constrains the property space of acetylcholine, the constraints appear-

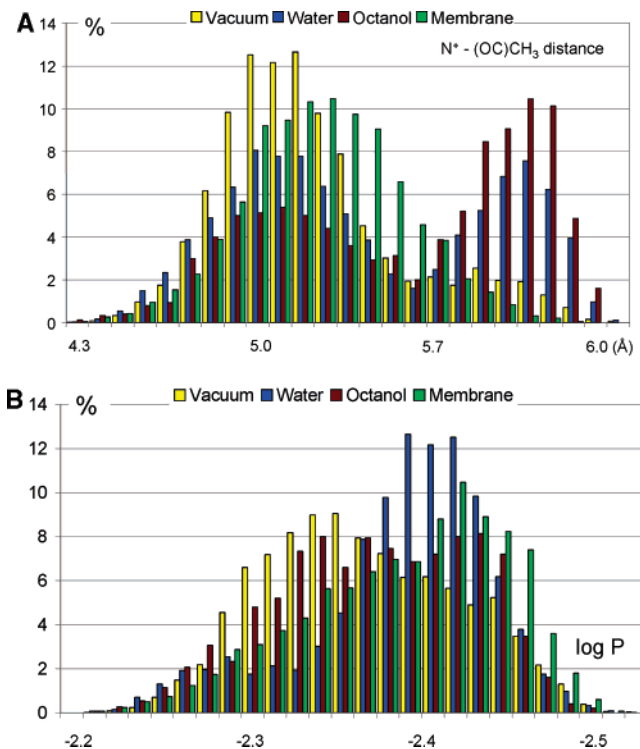


Figure 6. Histograms of some properties of acetylcholine conformers in a vacuum (yellow), in water (blue), in hydrated octanol (purple), and in a membrane (green). A: Distribution of (N^+) to (OC) CH_3 distances (10 bins/unit). B: Distribution of logP values (50 bins/unit). Note that the higher lipophilicity values are on the left.

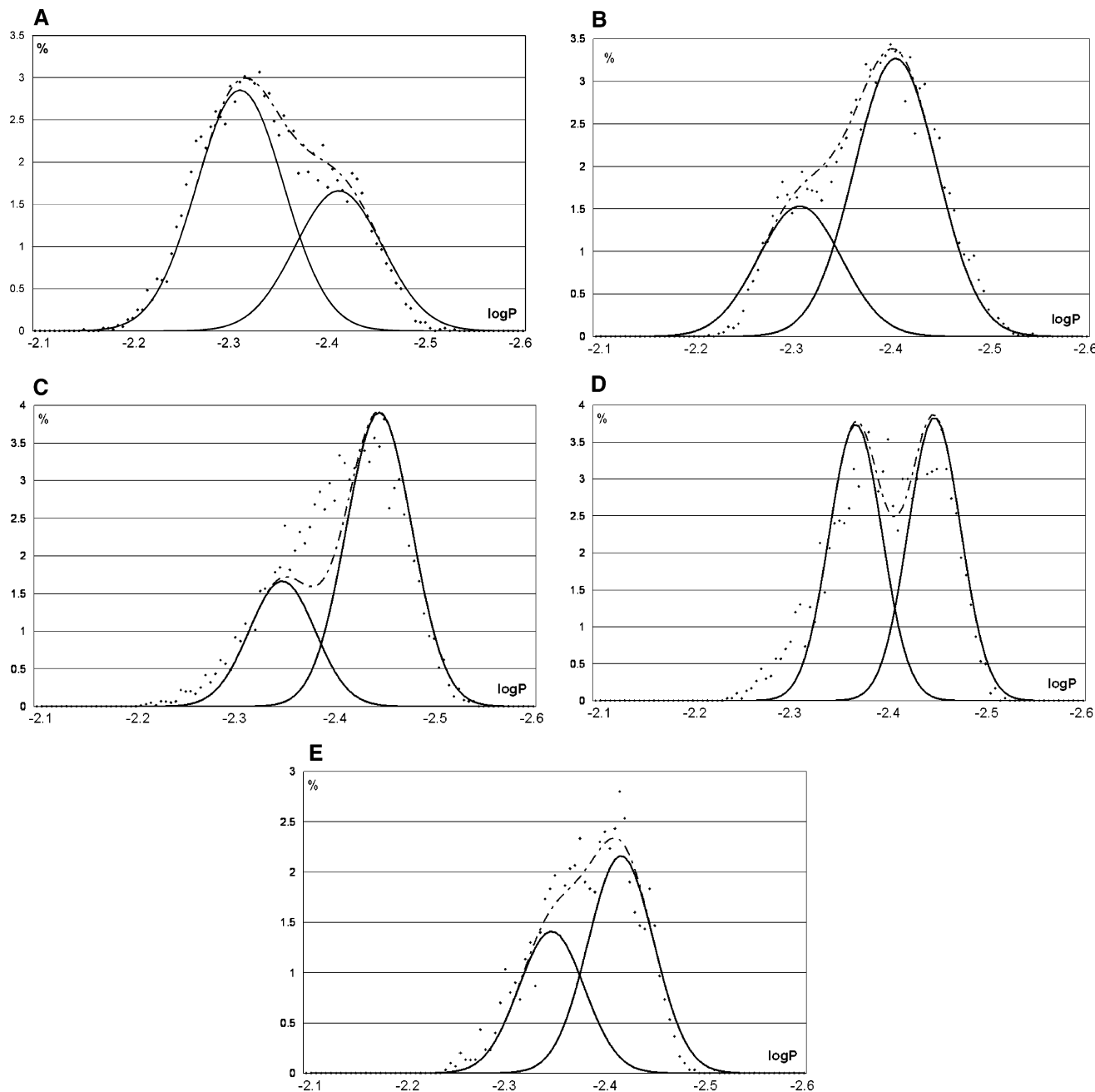
ing quite modest when comparing mean values. While the differences are generally significant between a vacuum and other media, they become very small when comparing the various solvents and cannot lead to meaningful conclusions. Histograms of property distributions represent a more informative approach and clearly reveal differences in solvent effects (Figure 6). Thus, the distances between (N^+) and (OC) CH_3 in the various media (Figure 6A) show a bimodal distribution, with the first peak being centered around 5.1–5.2 Å and the second around 5.9–6.0 Å. The distribution in octanol confirms that the peak corresponding to extended conformers is the most populated, whereas the distribution of distances in a membrane shows only the peak corresponding to folded forms, with extended conformers all but absent.

In contrast, bimodal distributions are less clear-cut in the histograms of lipophilicity space (Figure 6B), thus confusing solvent effects. Nevertheless, the histograms are suggestive of overlapping peaks. To examine this hypothesis, new histograms were first constructed using 100 bins rather than the 25 bins in Figure 6B and were deconvoluted into Gaussian-type peaks as explained under Methods. This deconvolution into two Gaussian-type curves proved successful, as demonstrated by the good quality of the statistics reported in Table 5. Figures 7 show the deconvoluted bimodal distributions of the lipophilicity space in all five media, whereas Table 5 also compares the characteristics (position and relative areas of peaks) of the Gaussian curves so obtained. One notes that the X-positions of the peaks are comparable in all distributions, with the more hydrophilic peaks in

Table 5. Statistics and Parameters of the Two Gaussian Curves Obtained by Deconvolution of the Histograms of Lipophilicity Spaces (see Figures 7)

medium	fitting parameters		hydrophilic peak			lipophilic peak		
	r^2	SD	center ^a	Y_{\max} ^b	area, % ^c	center ^a	Y_{\max} ^b	area, % ^c
vacuum	0.985	0.12	-2.41	1.66	36.8	-2.31	2.85	63.2
chloroform	0.981	0.16	-2.42	3.26	67.0	-2.32	1.53	33.0
water	0.928	0.32	-2.44	3.95	72.4	-2.34	1.66	27.6
octanol	0.912	0.38	-2.44	3.83	50.6	-2.37	3.74	49.4
membrane	0.960	0.17	-2.42	2.16	60.5	-2.34	1.41	39.5

^a logP values. ^b Maximal height of histogram peak in %. ^c Hydrophilic + lipophilic peak = 100%.

**Figure 7.** Deconvoluted bimodal distribution (Gaussian curves, see Table 5 for data) of lipophilicity spaces. The dots are the individual bins (100 for each medium), the broken lines are the calculated deconvolutions, and the continuous lines the calculated Gaussians: A: in a vacuum; B: in chloroform; C: in water; D: in hydrated *n*-octanol; E: in a membrane model.

the range -2.41 to -2.44, and the more lipophilic peaks in the range -2.31 to -2.37.

The real differences between media, and this is where our analysis becomes quite revealing, are in the relative areas of the two Gaussians. Indeed, the relative area of the more lipophilic peak decreases markedly in the

order vacuum > octanol > membrane > chloroform > water. This is in clear relation with the increasing polarity of the simulated media.

It is of interest to note that in all media there is little or no correspondence between geometry (folded vs extended conformers, Table 1) and lipophilicity (more

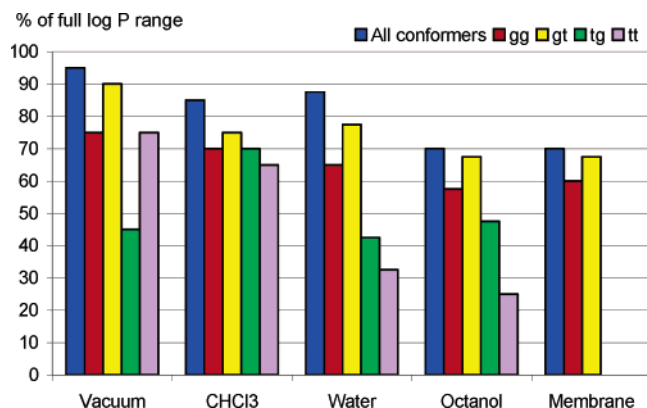


Figure 8. Percent of the full lipophilicity range (i.e., 0.40 in the logP scale) covered by the conformational clusters of acetylcholine in the various media investigated here and in a previous work.¹² Blue = all conformers; red = the +g+g and -g-g clusters; yellow = the +gt and -gt clusters; green = the t+g and t-g clusters; violet = the tt cluster.

lipophilic vs more hydrophilic conformers, Table 5) and that only in a vacuum is the lipophilic peak more abundant than the hydrophilic one. This result offers compelling evidence that conformational space and property spaces are only partly interdependent and that each conformational cluster can span a large portion of property space, as already suggested by the data in Table 3C. This conclusion is confirmed by the bimodal lipophilicity distribution in a membrane, where one observes two distinct deconvoluted Gaussians despite the fact that acetylcholine is entirely constrained in folded conformations. Figure 7 also suggests that deconvolution algorithms can be a tool of broad applicability to extract meaningful information from a fuzzy distribution of computed property values.

The capacity for acetylcholine to retain much of its lipophilicity range despite conformational constraints is best illustrated by the relative logP ranges covered by the various conformational clusters. The full logP range of the compound, as observed in our studies, is 0.40 (from one extreme of -2.55 in water as the most polar environment to the other extreme of -2.15 in a vacuum as the most apolar environment). As seen in Figure 8, the gg clusters cover between 58 and 75% of this range, whereas the gt clusters cover between 68 and 90%, the tg clusters between 42 and 75%, and the tt cluster between 25 and 75% depending on the medium. This indicates that each conformational cluster includes pools of more lipophilic and more hydrophilic conformers, and that the medium selects (extracts) from each conformational cluster those conformers that best resemble its own polarity.

Conclusion

The analysis of conformational space and property spaces as computed in all media considered (namely a vacuum, chloroform, water, octanol, and a membrane) leads to some significant considerations. The simulated media can be classified in three groups: chloroform and water are disordered, isotropic media formed from small molecules; octanol is a more ordered, isotropic, higher-size medium, and may even be considered anisotropic at the atomic level; finally, a membrane is a well-ordered yet fluid anisotropic medium.

The two isotropic media (chloroform and water) similarly influence the conformational space of acetylcholine. Compared to a vacuum, the isotropic media whatever their polarity allow for a marked fraction of extended conformers, but the folded ones predominate since they minimize friction with the solvent. In a more complex, higher-size medium such as hydrated *n*-octanol, the conformational space is under increased constraint as the solute also tries to mimic the shape of the solvent to minimize steric repulsion. In a genuinely anisotropic medium such as a membrane, the conformational space of acetylcholine is strongly constrained to almost exclusively folded forms.

As a general trend, acetylcholine adapts its property spaces to the surrounding medium, with apolar media favoring the lesser polar (more lipophilic) conformers, and polar media having the opposite effect. In isotropic media (namely chloroform, water, and octanol) this mimicry in polarity is obtained not by major conformational constraints, but because the medium selects from the various conformational clusters those conformers whose polarity most resembles its own. This is made possible by the facts uncovered here: (a) that the conformational and property spaces are partly independent from each other, and (b) that each conformational cluster can access a large fraction of the property spaces of the solute.

A point of interest is whether the stronger constraints on the property space of acetylcholine seen in a membrane are due to the disappearance of some conformational clusters. As shown in this work, the disappearance of extended forms in a membrane does not prevent acetylcholine to access about 2/3 of its full lipophilicity range (Figure 8). The simulations reported here suggest that in all media, acetylcholine tends to preserve much of its full conformational and property spaces. Entropic factors appear involved, but more work is needed to clarify this question.

Overall, this and previous simulations^{12,16} illustrate the complexity of solute-solvent interactions. They reveal quantitative information on the level of constraints experienced by solutes, and they bring further evidence of the adaptability of biomolecules to their environment.^{28,29} Work in progress further indicates that explorations of the property spaces of bioactive molecules may lead to new and promising tools in dynamic QSARs.³⁰

Methods

Conformational Properties of Acetylcholine. The initial geometry of acetylcholine was constructed and energy-minimized using the Quanta/CHARMm package (MSI, Burlington, MA). The computation of partial atomic charges and the final geometry optimization were carried out at the semiempirical level with the MOPAC 6.0 program (keywords = AM1, PRECISE, GEO-OK).³¹

Acetylcholine has four dihedral angles (Figure 1), but τ_1 and τ_4 vary in a narrow range and independently of the conditions ($\tau_1 = 60^\circ \pm 20^\circ$; and $\tau_4 = 0^\circ \pm 20^\circ$) due to the symmetry of the triple rotor τ_1 and to the rigidity of the ester group (τ_4). Our previous studies revealed seven low-energy conformational clusters for acetylcholine.^{12,26} The present work does not focus on relative conformational energies, hence all conformers having τ_2 and/or τ_3 in an *anticlinal* conformation were considered as transition forms.

Construction of a Membrane Model. The phospholipid bilayer was built using a unity cell composed by two molecules of (*R*)-1-palmitoyl-2-oleoyl-sn-glycero-3-phosphocholine (POPC). The POPC molecule was built in its favored *zigzag* conformation, energy-minimized and optimized using MOPAC 6.0 with partial charges calculation. The two opposite POPC molecules were arranged with an overlap of about 12 Å among aliphatic chains, to maximize hydrophobic interactions. A fluid phospholipid bilayer model was obtained, which was characterized by a remarkable flexibility and a thickness of 50 Å (1/4 corresponding to overlapped POPC chains, 2/4 to nonoverlapping chains, and 1/4 to the POPC headgroups). The unity cell was further optimized with MOPAC 6.0 and multiplied in the *X* and *Y* directions (*X* = 8, *Y* = 8, *Z* = 1) using the cluster builder in VEGA.³² The square parallelepiped so obtained contained 128 POPC residues (85 Å × 85 Å × 50 Å, 6656 heavy atoms) and was minimized (RMS = 0.01) in order to optimize intermolecular interactions.

The water layers were arranged by cutting two bands of TIP3S water molecules each containing 8760 solvent residues (85 Å × 85 Å × 40 Å) and manually locating them over and under the phospholipid segment. The complex was minimized (RMS = 0.1) and underwent 1 ns MD simulation to allow some water molecules to permeate the polar headgroup regions.

Molecular Dynamics Simulations. All calculations were carried out in a dual Athlon PC. The package Namd2.51³³ was used with the force-field CHARMM v22. The initial structure of acetylcholine for all simulations was the +g+g geometry. A previous study²⁶ had shown that the nature of the starting conformer had no influence of the results. The cluster of hydrated octanol was built as described in previous study.²⁶ For simulations in hydrated octanol a solvent sphere with a radius of 15 Å around the solute was used, and a spherical boundary condition (radius = 28 Å) was applied to stabilize the octanol cluster.

For the simulations in the membrane model, acetylcholine was inserted into a membrane segment of dimensions 20 Å × 20 Å × 60 Å. The height of this square parallelepiped (60 Å) corresponds to a complete POPC bilayer (50 Å) plus two external water layers of 5 Å. The molecule of acetylcholine was placed in the center of this cluster and cylindrical boundary conditions (radius = 20 Å, height = 60 Å) were applied to stabilize the solvent molecules.

Before performing the MD simulations, both complexes were also optimized for the relative position of the solvent molecules to eliminate any high-energy interaction. The simulations were carried out for 15 ns in hydrated octanol and in the membrane model. No constraint was imposed on any of the dihedral angles, but only τ_2 and τ_3 were monitored. It is interestingly to note that acetylcholine approached the POPC headgroups already during the MD equilibration period, and that it did remain there during the entire duration (15 ns) of the simulation.

All simulations had the following characteristics: minimizations with the conjugate gradients algorithm, convergence limit (RMS) = 0.01, maximal number of iterations = 5000; molecular dynamics with constant temperature in the range 300 ± 25 K, integration of Newton's equation each 1 fs according to Verlet's algorithm, frame stored each 5000 iterations (5.0 ps), yielding 3000 frames per trajectory. The molecular dynamics were carried out in three phases: an initial period of heating from 0 to 300 K over 3000 iterations (3 ps, i.e., 1 K/10 iterations), an equilibration period of 3 ns, and the monitored phase of simulation of 15 ns. Only frames memorized during this third phase were considered.

Computation of Geometric and Physicochemical Properties of Conformers. The results of the MD simulations were analyzed with VEGA.³² The geometric parameters include the dihedral angles τ_2 and τ_3 as defined in Figure 1, and the distance between the N⁺ atom and the methyl C8 atom (Figure 1), as this is intuitively suitable to assess the degree of folding of acetylcholine. The virtual logP was calculated by the MLP tool.⁸ The SAS was calculated with a solvent molecule of radius equal to 1.4 Å. The PSA was calculated by subtracting

the contributions of carbon and nonpolar hydrogen atoms from the SAS.³⁴ The logP distributions were deconvoluted into Gaussian-type peaks by means of a FFT filtering smoothing using PeakFit 4.12 (Systat/Seasolve, Richmond, CA).

References

- (1) Dobson, C. M. Chemical space and biology. *Nature* **2004**, *432*, 824–828.
- (2) Feher, M.; Schmidt, J. M. Property Distributions: Differences between Drugs, Natural Products, and Molecules from Combinatorial Chemistry. *J. Chem. Inf. Comput. Sci.* **2003**, *43*, 218–227.
- (3) Testa, B.; Kier, L. B.; Carrupt, P. A. A systems approach to molecular structure, intermolecular recognition, and emergence-dissolution in medicinal research. *Med. Res. Rev.* **1997**, *17*, 303–326.
- (4) Burgen, A. S. V. Conformational changes and drug action. *Fed. Proc.* **1981**, *40*, 2723–2728.
- (5) Klyne, W.; Prelog, V. Description of steric relationships across single bonds. *Experientia* **1960**, *17*, 521–523.
- (6) Carrupt, P. A.; El Tayar, N.; Karlén, A.; Testa, B. Value and limits of molecular electrostatic potentials for characterizing drug-biosystem interactions. *Methods Enzymol.* **1991**, *203*, 638–677.
- (7) Carrupt, P. A.; Testa, B.; Gaillard, P. Computational approaches to lipophilicity: Methods and applications. *Rev. Comput. Chem.* **1997**, *11*, 241–315.
- (8) Gaillard, P.; Carrupt, P. A.; Testa, B.; Boudon, A. Molecular lipophilicity potential, a tool in 3D-QSAR. Method and applications. *J. Comput.-Aided Mol. Des.* **1994**, *8*, 83–96.
- (9) Rey, S.; Caron, G.; Ermondi, G.; Gaillard, P.; Pagliara, A.; Carrupt, P. A.; Testa, B. Development of Molecular Hydrogen Bonding Potentials (MHBPs) and their application to structure-permeation relations. *J. Comput.-Aided Mol. Des.* **2001**, *19*, 521–535.
- (10) Tsai, R. S.; Carrupt, P. A.; Testa, B.; El Tayar, N.; Grunewald, G. L.; Casy, A. F. Influence of stereochemical factors on the partition coefficient of diastereomers in a biphasic octan-1-ol/water system. *J. Chem. Res.* **1993**, 1901–1920.
- (11) Kraszni, M.; Bányai, I.; Noszál, B. Determination of conformer-specific partition coefficients in octanol/water systems. *J. Med. Chem.* **2003**, *46*, 2241–2245.
- (12) Vistoli, G.; Pedretti, A.; Villa, L.; Testa, B. Solvent constraints on the property space of acetylcholine. I. Isotropic solvents. *J. Med. Chem.* **2005**, *48*, 1759–1767.
- (13) Chothia, C.; Pauling, P. J. Conformation of cholinergic molecules relevant to acetylcholinesterase. *Nature* **1969**, *223*, 919–921.
- (14) Partington, P.; Feeney, J.; Burgen, A. S. V. The conformation of acetylcholine and related compounds in aqueous solution as studied by NMR spectroscopy. *Mol. Pharmacol.* **1972**, *8*, 269–277.
- (15) Genson, D. W.; Christoffersen, R. E. Ab initio calculations on large molecules using molecular fragments. Electronic and geometric characterization of acetylcholine. *J. Am. Chem. Soc.* **1973**, *95*, 362–368.
- (16) Beveridge, D. L.; Kelly, M. M.; Radna, R. J. A theoretical study of solvent effects on the conformational stability of acetylcholine. *J. Am. Chem. Soc.* **1974**, *96*, 3769–3778.
- (17) Gelin, B. R.; Karplus, M. Role of structural flexibility in conformational calculations. Application to acetylcholine and β -methylacetylcholine. *J. Am. Chem. Soc.* **1975**, *97*, 6996–7006.
- (18) Langlet, J.; Claverie, P.; Pullman, B.; Piazzola, D.; Daudey, J. P. Studies of solvent effects. III. Solvent effect on the conformation of acetylcholine. *Theor. Chim. Acta* **1977**, *46*, 105–116.
- (19) Cassidei, L.; Sciacovelli, O. Conformational analysis of the C(6)–O(1)–C(5)–C(4) fragment in acetylcholine by carbon-13 NMR spectroscopy. *J. Am. Chem. Soc.* **1981**, *103*, 933–934.
- (20) Margheritis, C.; Corongiu, G. Acetylcholine in water: Ab initio potential and Monte Carlo simulation. *J. Comput. Chem.* **1988**, *9*, 1–10.
- (21) Behling, R. W.; Yamane, T.; Navon, G.; Jelinsky, L. W. Conformation of acetylcholine bound to the nicotinic acetylcholine receptor. *Proc. Natl. Acad. Sci. U.S.A.* **1988**, *85*, 6721–6725.
- (22) Kim, Y. J.; Kim, S. C.; Kang, Y. K. Conformation and hydration of acetylcholine. *J. Mol. Struct.* **1992**, *269*, 231–241.
- (23) Segall, M. D.; Payne, M. C.; Boyes, R. N. An ab initio study of the conformational energy map of acetylcholine. *Mol. Phys.* **1998**, *93*, 365–370.
- (24) Williamson, P. T. F.; Watts, J. A.; Addona, G. H.; Miller, K. W.; Watts, A. Dynamics and orientation of N+(CD3) β -bromoacetylcholine bound to its binding site on the nicotinic acetylcholine receptor. *Proc. Nat. Acad. Sci. U.S.A.* **2001**, *98*, 2346–2351.
- (25) Marino, T.; Russo, N.; Toci, E.; Toscano, M. Molecular dynamics, density functional and second-order Moller–Plesset theory study

- of the structure and conformation of acetylcholine in vacuo and in solution. *Theor. Chem. Acc.* **2001**, *107*, 8–14.
- (26) Vistoli, G.; Pedretti, A.; Villa, L.; Testa, B. The solute–solvent system: Solvent constraints on the conformational dynamics of acetylcholine. *J. Am. Chem. Soc.* **2002**, *124*, 7472–7480.
- (27) Dutt, G. B. Molecular rotation as a tool for exploring specific solute–solvent interactions. *ChemPhysChem* **2005**, *6*, 413–418.
- (28) Jiang, X.-K. Hydrophobic-lipophilic interactions. Aggregation and self-coiling of organic molecules. *Acc. Chem. Res.* **1988**, *21*, 362–367.
- (29) Rabitz, H. Systems analysis at the molecular scale. *Science* **1989**, *246*, 221–226.
- (30) Vistoli, G.; Pedretti, A.; Villa, L.; Testa, B. Range and Sensitivity as Descriptors of Molecular Property Spaces in Dynamic QSAR Analyses. *J. Med. Chem.* **2005**, *48*, 4947–4952.
- (31) Bredow, T.; Jug, K. Theory and range of modern semiempirical molecular orbital methods. *Theor. Chem. Acc.* **2005**, *113*, 1–14
- (32) Pedretti, A.; Villa, L.; Vistoli, G. VEGA: a versatile program to convert, handle and visualize molecular structure on windows-based PCs. *J. Mol. Graph.* **2002**, *21*, 47–49.
- (33) Kalé, L.; Skeel, R.; Bhandarkar, M.; Brunner, R.; Gursoy, A.; Krawetz, N.; Phillips, J.; Shinozaki, A.; Varadarajan, K.; Schulten, K. NAMD2: Greater scalability for parallel molecular dynamics. *J. Comput. Phys.* **1999**, *151*, 283–312.
- (34) Veber, D. F.; Johnson, S. R.; Cheng, H. Y.; Smith, B. R.; Ward, K. W.; Kopple, K. D. Molecular properties that influence the oral bioavailability of drug candidates. *J. Med. Chem.* **2002**, *45*, 2615–2623.

JM0580306